SLAC-PUB-654
August 1969
(EXP) (TH)

PRODUCTION OF ρ^{o} MESONS BY LINEARLY POLARIZED PHOTONS AT 2.8 AND 4.7 GEV*

J. Ballam, G.B. Chadwick, R. Gearhart, Z.G.T. Guiragossián, M. Menke, J.J. Murray, P. Seyboth,** A. Shapira,*** I.O. Skillicorn,**** G. Wolf†
Stanford Linear Accelerator Center
Stanford University, Stanford, California 94305

R.H. Milburn†† and C.K. Sinclair
Tufts University, Medford, Massachusetts 02155

H.H. Bingham, W.B. Fretter, W.R. Graves, K.C. Moffeit, W.J. Podolsky, M.S. Rabin, A.H. Rosenfeld, and R. Windmolders†††
Department of Physics and Lawrence Radiation Laboratory
University of California, Berkeley, California 94720

ABSTRACT

Interactions of laser-induced ~95% linearly polarized photons in the 82-inch hydrogen bubble chamber at SLAC have been examined to study ρ^{o} photoproduction via $\gamma p \rightarrow \rho^{o} p$. Based on a sample of about 1500 ρ^{o} events at 2.8 and 4.7 GeV beam energies, results are given on the total channel cross section and the momentum transfer distribution. The ρ^{o} decay spin density matrix elements are examined in the presence of polarization correlations. A strong azimuthal correlation with respect to the photon polarization is observed in the ρ^{o} decay.

(International Symposium on Electron and Photon Interactions at High Energies, Daresbury, England, Sept. 1969)

*Work supported in part by the U.S. Atomic Energy Commission and the National Science Foundation.

**On leave from Max-Planck Institut für Physik and Astrophysick, Munich, Germany.

***On leave from Weizmann Institute of Science, Rehovot, Israel.

****On leave from Brookhaven National Laboratory, New York.

†On leave from Deutsches Elektronen-Synchrotron, Hamburg, Germany.

††Presently visitor at the Lawrence Radiation Laboratory, Berkeley, California.

†††On leave from Laboratoire Interuniversitaire des Hautes Energies, Brussels, Belgium.

We have investigated the ρ^o photoproduction process with linearly polarized photon beams at 2.8 and 4.7 GeV energies using the 82-inch hydrogen bubble chamber at SLAC. The laser induced photon beam is almost monochromatic and highly polarized.[1] The full widths at half maximum of the beam energy spectra are found[1] to be 0.150 and 0.300 GeV, respectively, with photon linear polarization of ~95 percent.

The total exposure amounts to ~810,000 pictures. Of these, one third have been completely analyzed, corresponding to 37 events/μb and 44 events/μb at 2.8 and 4.7 GeV, respectively. The overall scanning efficiency after double-scan and a third resolve-scan is more than 99 percent. The total number of hadronic events successfully processed is 13,220; of these 63.5 percent have three charged outgoing particles. We find 1157 acceptable 3C fits at 2.8 GeV and 866 such events at 4.7 GeV which satisfy the beam energy criteria and are of the type:

$$\gamma p \rightarrow p\pi^+\pi^- \qquad (1)$$

Figure 1 (a) and 1(b) show the Dalitz plot distributions for events of reaction (1). A strong ρ^o signal and some Δ^{++} production is observed.

Figure 2(a) and 2(b) show the $\pi^+\pi^-$ mass spectra from reaction (1) at 2.8 and 4.7 GeV, respectively. The measurement of the ρ^o photoproduction cross section from reaction (1) requires a knowledge of competing processes and the shapes of resonances. A maximum likelihood fit has been made to the data assuming Breit-Wigner p-wave resonance shapes[2] for ρ^o and Δ^{++} photoproduction in addition to phase space. The ρ^o shape is modified by the factor of $(m_\rho/m_{\pi\pi})^4$, as suggested by Ross and Stodolksy.[3] The curves in Fig. 2(a) and 2(b) show the results of these fits. The parameter values are summarized in Table 1.

TABLE 1

k (GeV)	m_ρ (MeV)	Γ_ρ (MeV)	Percentage of ρ^o	Percentage of Δ^{++}	σ_ρ (μb)	σ_Δ (μb)	σ(μb) $p\pi^+\pi^-$
2.8	765±5	152±11	64±4	13.5±3.0	20.1±1.2	4.2±1	31.4±1.5
4.7	753±4	134±8	76±4	7±2	15.2±0.7	1.4±0.6	20±1

A recently proposed ρ^o-ω interference model[4] not using the factor $(m_\rho/m_{\pi\pi})^4$ of Ross and Stodolsky, does not reproduce the $\pi^+\pi^-$ mass distribution if a value near 760 MeV is used for m_{ρ^o}.

The differential cross section for $\gamma p \to \rho^o p$ is obtained by dividing the data of reaction (1) into intervals in t, the square of the four-momentum transfer between incoming and outgoing nucleons, where within each t-interval we solve for the number of ρ^o's, using the maximum likelihood technique described above. The forward ρ^o photoproduction cross sections are obtained from a subsequent exponential fit, of the form $Ce^{-A|t|}$, to the t distributions seen in Fig. 3(a) and 3(b), for $|t| < 0.5$ $(GeV/c)^2$. For $d\sigma/dt(\gamma p \to \rho^o p)$ at $t = 0$, the values are 151 ± 15 $\mu b/(GeV/c)^2$ at 2.8 GeV and 115 ± 10 $\mu b/(GeV/c)^2$ at 4.7 GeV. The exponential slopes are found to be 7.2 ± 0.4 $(GeV/c)^{-2}$ at 2.8 GeV and 7.0 ± 0.5 $(GeV/c)^{-2}$ at 4.7 GeV.

The coordinate system, used in the analysis of ρ^o decay intensity distributions by linearly polarized photons, is given in Fig. 4. The production plane of $\gamma p \to \rho^o p$ contains the x-z axes. Depending upon the quantization axis, the angles θ and ϕ are the usual Jackson system or helicity system polar and aximuthal angles of the decay positive pion in the ρ^o rest frame. The angles Φ and ψ define the relative orientation of the production and decay planes with respect to the beam photon polarization. With these definitions, the azimuthal angles are related by $\psi_J = \phi_J + \Phi - 2\pi$. The ρ^o decay intensity distribution is analyzed in terms of nine parameters, using the following most general[5] normalized functional form, for linearly polarized photons:

$$I(\theta, \phi, \Phi) = \frac{1}{2\pi} \cdot \frac{3}{4\pi} \Bigg\{ \Big[\frac{1}{2}\left(1-\rho^{(0)}_{00}\right) + \frac{1}{2}\left(3\rho^{(0)}_{00}-1\right)\cos^2\theta - \rho^{(0)}_{1-1}\sin^2\theta \cos 2\phi$$

$$- 2\sqrt{2}\,\mathrm{Re}\rho^{(0)}_{10} \sin\theta \cos\theta \cos\phi \Big]$$

$$- P\cos 2\Phi \Big[\rho^{(1)}_{00}\cos^2\theta + \rho^{(1)}_{11}\sin^2\theta - \rho^{(1)}_{1-1}\sin^2\theta\cos 2\phi$$

$$- 2\sqrt{2}\,\mathrm{Re}\rho^{(1)}_{10}\sin\theta\cos\theta\cos\phi\Big]$$

$$+ P\sin 2\Phi\Big[\mathrm{Im}\rho^{(2)}_{1-1}\sin^2\theta\sin 2\phi + 2\sqrt{2}\,\mathrm{Im}\rho^{(2)}_{10}\sin\theta\cos\theta\sin\phi\Big]\Bigg\} \qquad (2)$$

In this expresssion P refers to the percentage of beam linear polarization, for which we use the value of 95.6 percent at 2.8 GeV and 93.1 percent at 4.7 GeV, as computed from the backward Compton scattering process and our beam geometry. The generalized ρ^o spin density matrix elements $\rho^{(\lambda)}_{ik}$, in the $\lambda = 0$ case, correspond to the conventional p-wave boson decay formalism. The additional correlations introduced by the $\lambda = 1$ and 2 cases are due to the photon's linear polarization and together with the elements of $\lambda = 0$, can be used to derive relations to examine various production mechanisms. Among the most interesting realtions are the measure of ρ^o photoproduction polarization asymmetry $\Sigma = (\sigma_{\parallel} - \sigma_{\perp})/(\sigma_{\parallel} + \sigma_{\perp})$ and the parity exchange asymmetry $P_\sigma = (\sigma_+ - \sigma_-)/(\sigma_+ + \sigma_-)$. Here, $\sigma_{\parallel} = \sigma \cdot \bar{I}\left(\theta = \frac{\pi}{2},\ \phi = \frac{\pi}{2},\ \Phi = \frac{\pi}{2}\right)$ and $\sigma_{\perp} = \sigma \cdot I\left(\theta = \frac{\pi}{2}, \phi = \frac{\pi}{2},\ \Phi = 0\right)$ for $P_\gamma = 1$, $\sigma_+(\sigma_-)$ is the cross section for $\gamma p \to \rho^o p$ due to natural (unnatural) parity exchange mechanism. The relationships are[6]:

$$\Sigma = \frac{\sigma_{\parallel} - \sigma_{\perp}}{\sigma_{\parallel} + \sigma_{\perp}} = \frac{\rho_{11}^{(1)} + \rho_{1-1}^{(1)}}{\rho_{11}^{(0)} + \rho_{1-1}^{(0)}} \tag{3}$$

and

$$P_{\sigma} = \frac{\sigma_{+} - \sigma_{-}}{\sigma_{+} + \sigma_{-}} = 2\rho_{1-1}^{(1)} - \rho_{00}^{(1)} \tag{4}$$

A strong correlation between the photon polarization vector and ρ^{0} decay plane containing the quantization axis, is observed on the ϕ vs ψ scatter plots of Fig. 5. It is seen that the ρ^{0} decay plane is predominantly oriented along the photon's electric polarization direction. The behavior of the ρ^{0} polar and azimuthal decay angles θ and ϕ in the helicity frame are also shown in this figure. These are similar in behavior to those obtained in previous unpolarized photoproduction experiments.[7] The variations of $\rho_{ik}^{(0)}$, from the unpolarized part of the generalized decay distribution function are shown as a function of t in Fig. 6. This behavior is entirely consistent with previous experiments.

The polarization asymmetry in ρ^{0} photoproduction has been measured in a counter/spark chamber experimental setup at DESY.[8] Our measurement of Σ, using Eq. (3) and the complete determination of all parameters appearing in Eq. (2), is consistent with the DESY results. Figure 7(a) shows our determination of the ρ^{0} polarization asymmetry at 2.8 GeV, in comparison with the DESY results at 2.25 GeV. Figure 7(b) gives $\Sigma_{\rho}(t)$ at 4.7 GeV.

The cross sectional asymmetry between natural and unnatural parity exchange processes in $\gamma p \to \rho^{0} p$ can be measured using Eq. (4). Our results, given in Fig. 8, show that contributions from unnatural parity exchanges in $\gamma p \to \rho^{0} p$ are small at 2.8 and 4.7 GeV.

Finally, we have compared our results with a quark model prediction[9] that the statistical tensor[10] $\mathrm{Im}T_2^2$ vanish in a special reference system when the photon polarization vector is perpendicular to the scattering plane. In this system the quantization axis is normal to the $\gamma p \rightarrow \rho^o p$ production plane. In terms of our notation in Fig. 4, this condition corresponds to $\phi = \frac{\pi}{2}$ or $\frac{3\pi}{2}$. Figure 9 shows that this prediction is well satisfied. This statistical tensor is the expectation value of $- 5/4 < \sin^2\theta \ \sin 2\phi >$, evaluated in the special system.

REFERENCES

1. LRL-SLAC-TUFTS-UCB Collaboration, "Total and Partial Photoproduction Cross Sections at 1.44, 2.8 and 4.7 GeV," Report No. SLAC-PUB-618, Stanford Linear Accelerator Center, Stanford University (1969) (to be published).
2. J. D. Jackson, Nuovo Cimento 34, 1644 (1964).
3. M. Ross and L. Stodolsky, Phys. Rev. 149, 1172 (1966).
4. A. S. Goldhaber, G. C. Fox and C. Quigg, "The Barbarous ω Pierces the ρ^0 to Reveal a π-B Exchange Degeneracy," Report No. UCRL-19241, Lawrence Radiation Laboratory, University of California (1969) (to be published).
5. R. L. Thews, Phys. Rev. 175, 1749 (1968).
6. K. Schilling, P. Seyboth and G. Wolf, "On the Analysis of Vector Meson Production by Polarized Photons," (1969) (to be published).
7. Aachen-Berlin-Bonn-Hamburg-Heidelberg-München Collaboration, Phys. Rev. 175, 1669 (1969) (and references quoted therein).
8. L. Criegee *et al.*, Phys. Letters 28B, 282 (1968). (cf. also E. Lohrmann, Rapporteur's Talk, Lund Conference, June 1969).
9. B. Gorczca and M. Hayaski, "The Angular Decay Distributions of the Resonances Produced in the Photoproduction Processes $\gamma B \to VB$ and $\gamma B \to VB^*$ by the Quark Model," Report No. TPJU-4/69, Institute of Physics, Jagellonian University, Cracow (1969).
10. A. Kotanski and K. Zalewski, Nucl. Phys. B4, 559 (1968).

FIGURE CAPTIONS

1. Dalitz plot of $\gamma p \to p\pi^+\pi^-$ at (a) 2.8 GeV and (b) 4.7 GeV.
2. $\pi^+\pi^-$ mass spectrum from $\gamma p \to p\pi^+\pi^-$ at (a) 2.8 GeV and (b) 4.7 GeV. The superimposed curves are from a maximum likelihood fit including ρ^o, Δ^{++} and phase contributions.
3. Differential ρ^o cross section from $\gamma p \to p\pi^+\pi^-$ at (a) 2.8 GeV and (b) 4.7 GeV, obtained from maximum likelihood fits.
4. ρ^o decay analysis coordinate system in linearly polarized photoproduction.
5. Correlation between ρ^o decay plane and photon polarization. Distributions of polar and azimuthal helicity frame decay angles in (a) 2.8 GeV data and (b) 4.7 GeV data.
6. Behavior of the unpolarized part of ρ^o photoproduction spin density matrix elements, (a) at 2.8 GeV and (b) at 4.7 GeV.
7. (a) ρ^o photoproduction polarization asymmetry measurements at 2.8 GeV and comparison with the data of reference (7) at 2.25 GeV. (b) measurement of $\Sigma_\rho(t)$ at 4.7 GeV.
8. Parity exchange asymmetry distribution in $\gamma p \to \rho^o p$ at (a) 2.8 GeV and (b) 4.7 GeV.
9. Behavior of the statistical tensor Im T_2^2 as a function of Φ(folded), as compared with a quark model prediction of reference (9), in the Helicity, Jackson and Adair systems.

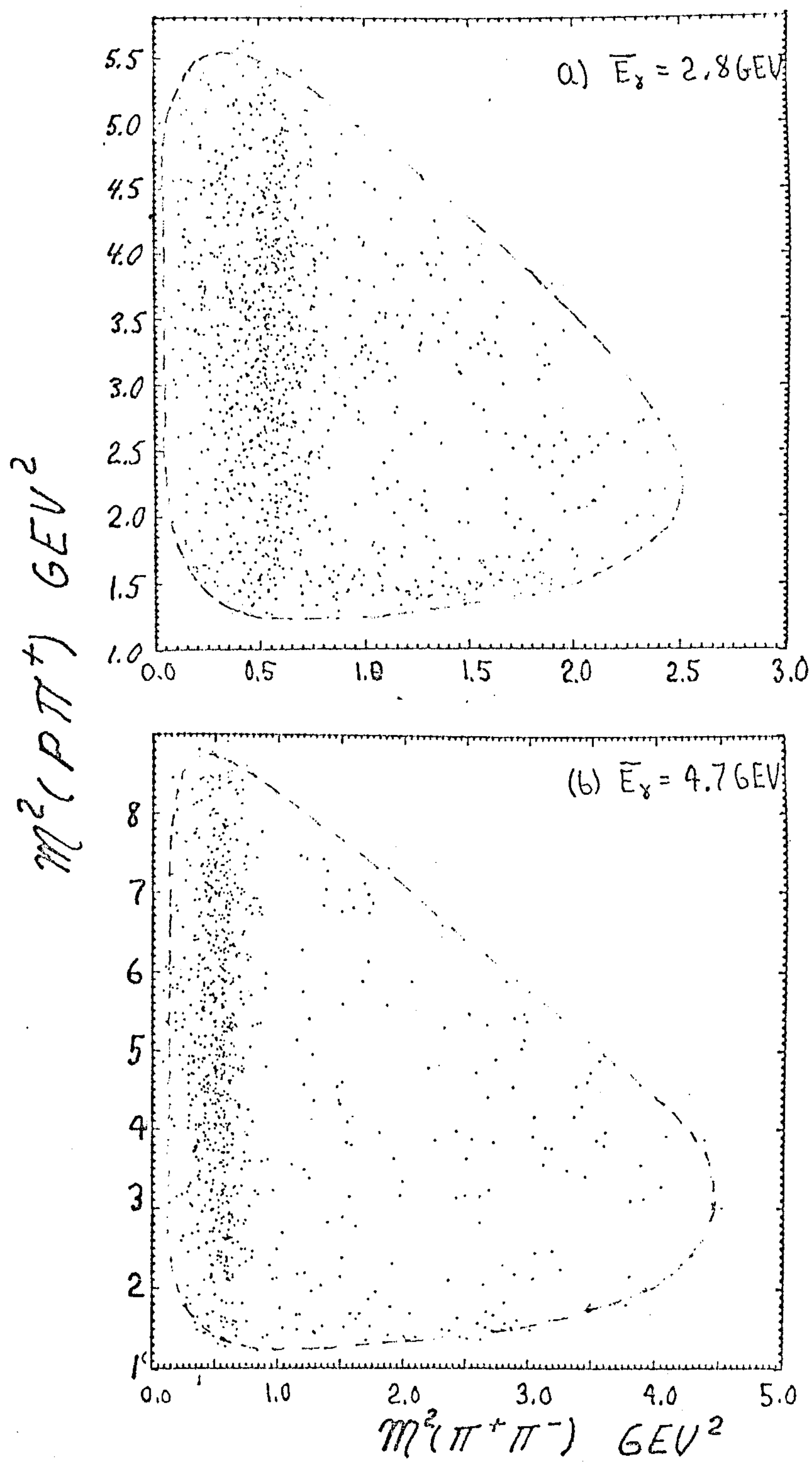

FIG. 1

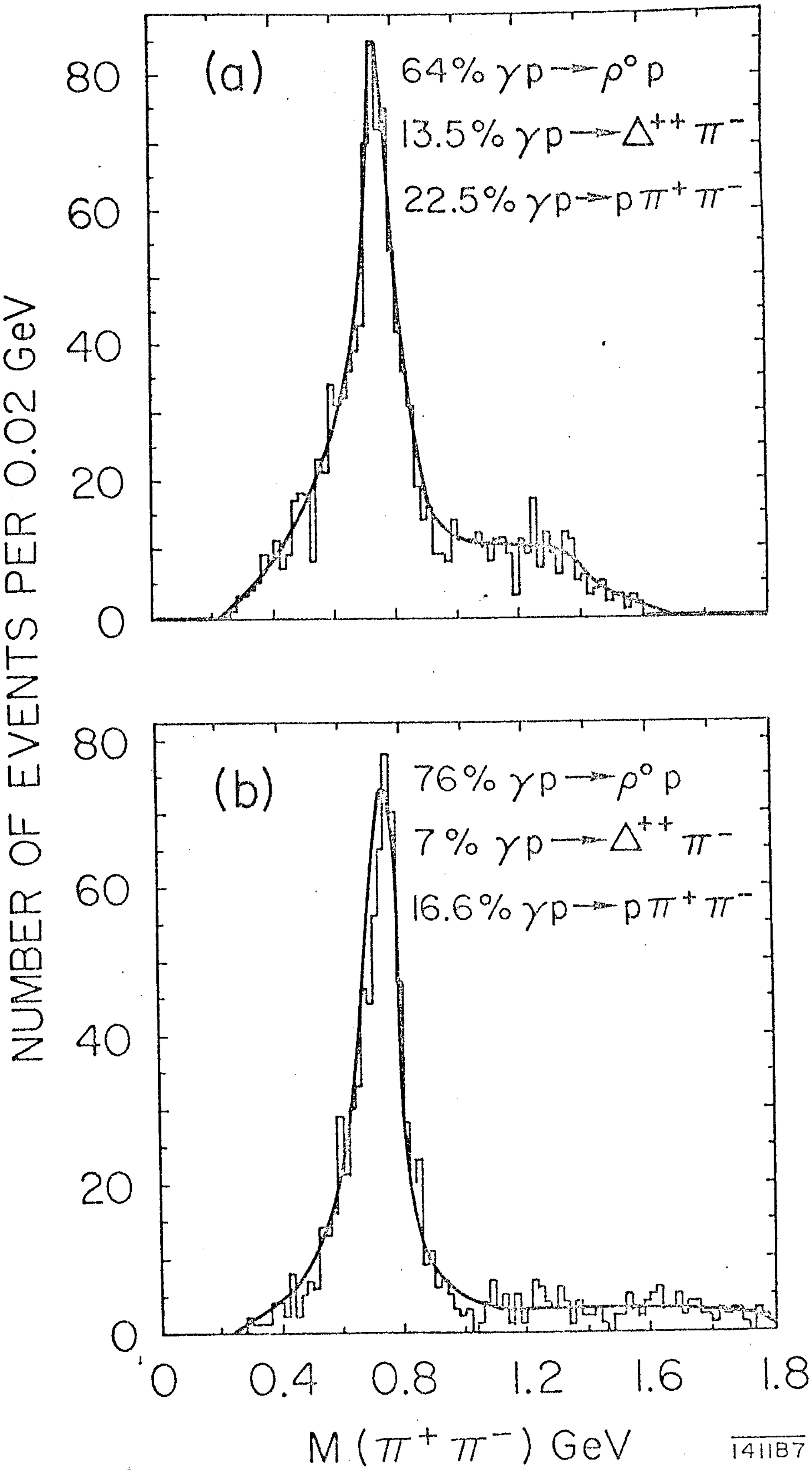

(a)
64% γp → ρ° p
13.5% γp → Δ++ π−
22.5% γp → pπ+π−
(b)
76% γp → ρ° p
7% γp → Δ++ π−
16.6% γp → pπ+π−
NUMBER OF EVENTS PER 0.02 GeV
M (π+π−) GeV
0
20
40
60
80
0.4
0.8
1.2
1.6
1.8
1411B7

FIG. 2

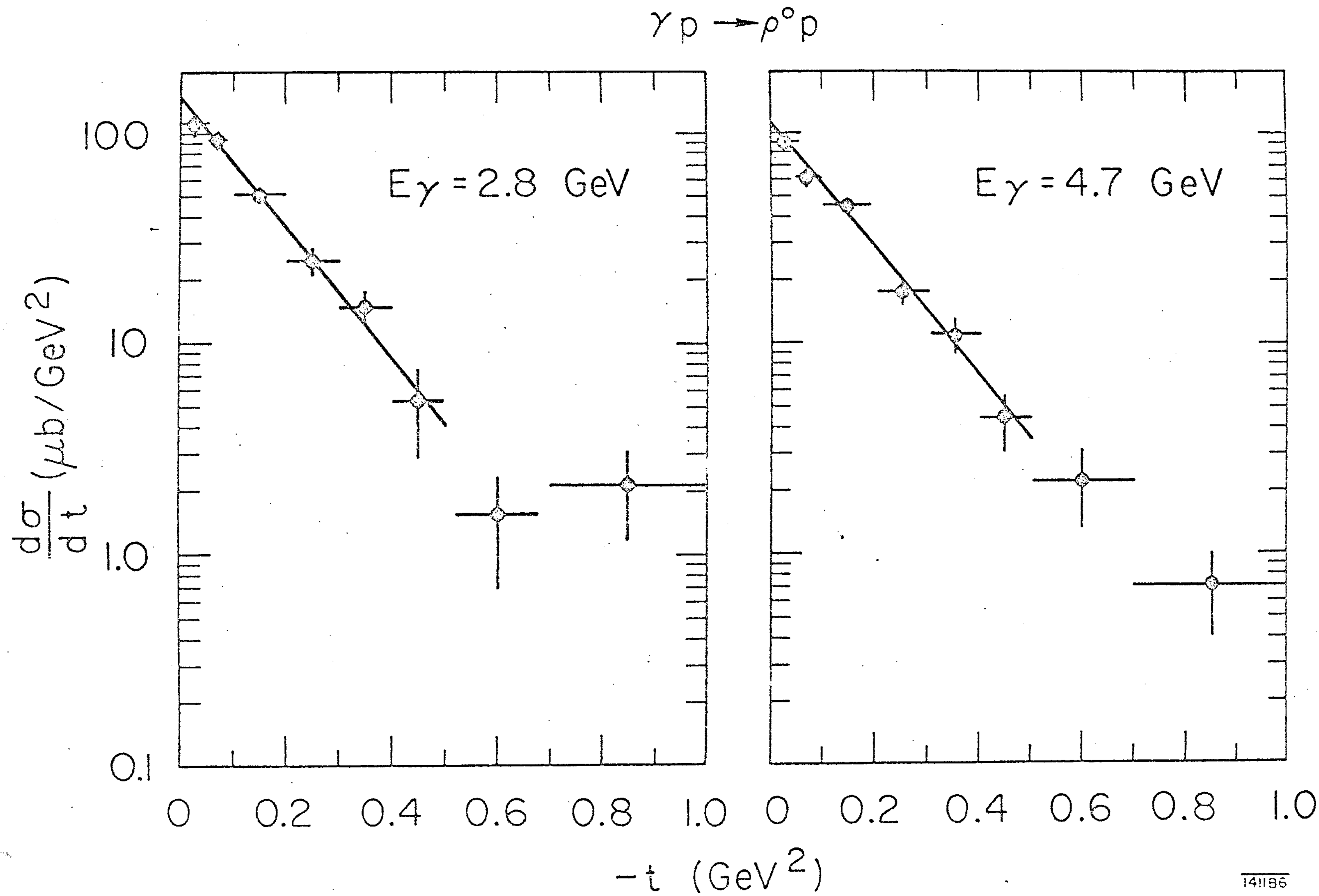
γp → ρ°p
Eγ = 2.8 GeV
Eγ = 4.7 GeV
dσ/dt (μb/GeV²)
100
10
1.0
0.1
0
0.2
0.4
0.6
0.8
1.0
−t (GeV²)
141186

FIG. 3

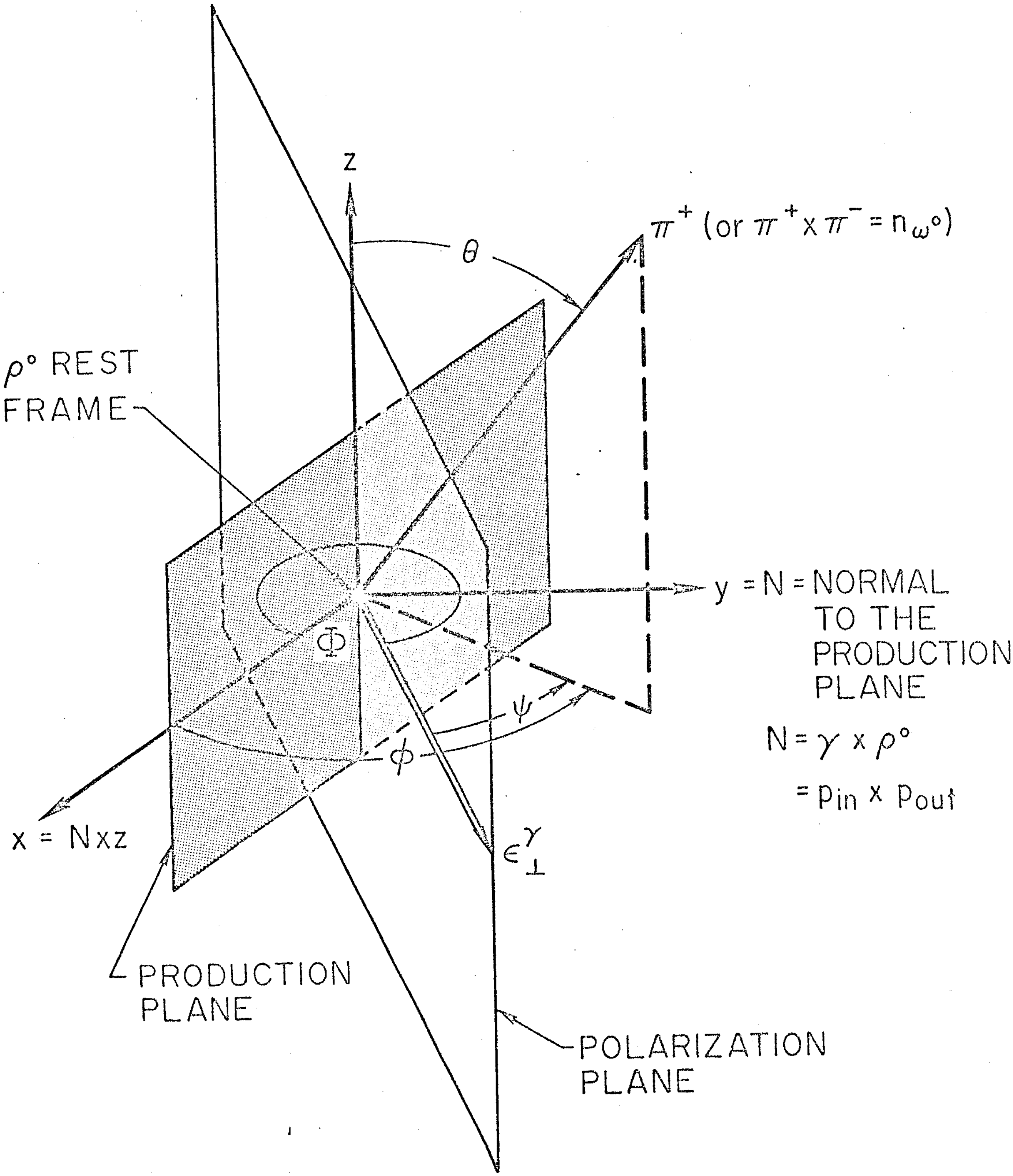
z
π^+ (or $\pi^+ \times \pi^- = n_{\omega^\circ}$)
θ
ρ° REST
FRAME
y = N = NORMAL
TO THE
PRODUCTION
PLANE
Φ
ψ
ϕ
$N = \gamma \times \rho^\circ$
$= p_{in} \times p_{out}$
x = N x z
$\epsilon_\perp^\gamma$
PRODUCTION
PLANE
POLARIZATION
PLANE

FIG. 4

1411A4

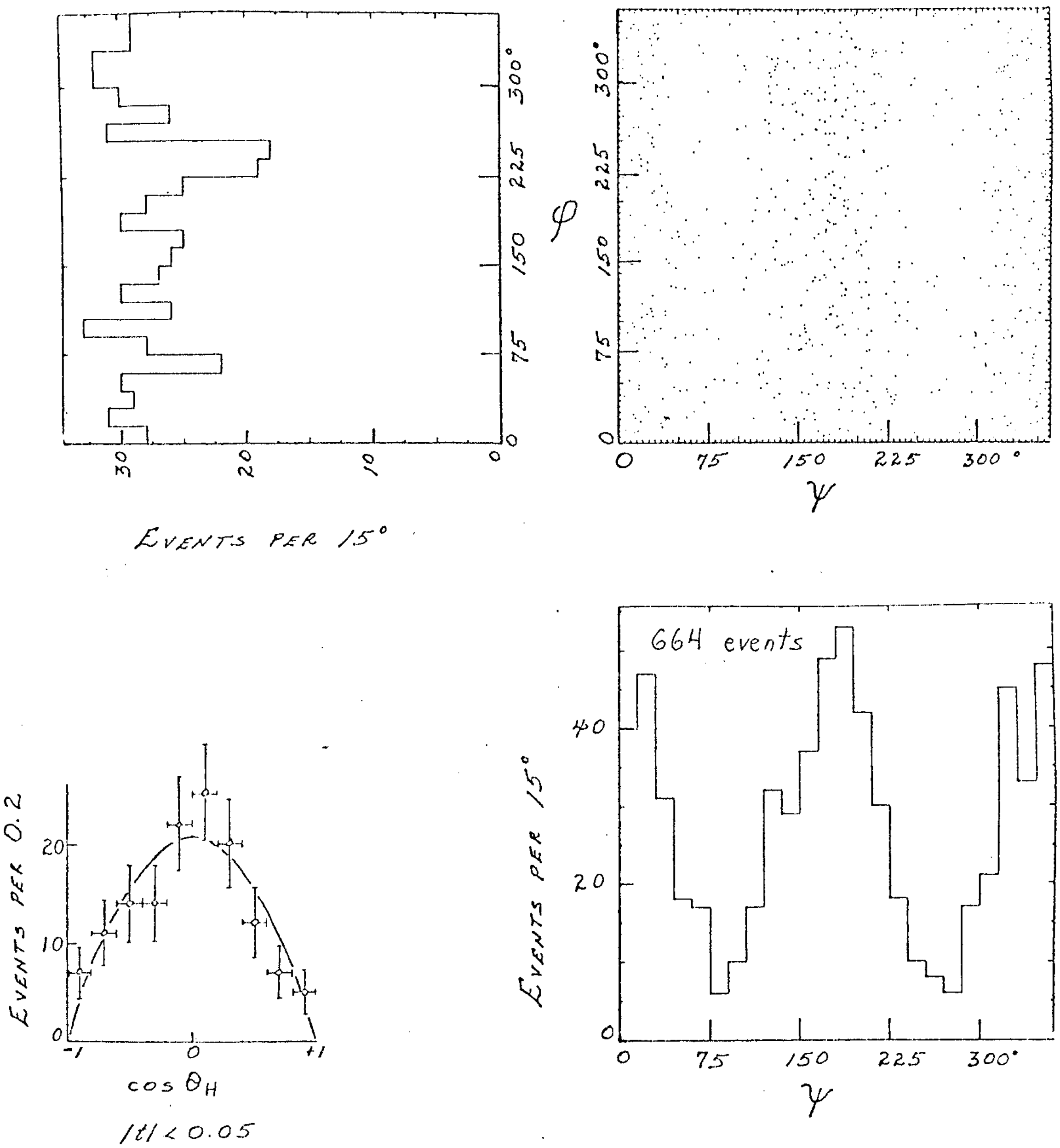

Fig 5a $\gamma p \to \rho^0 p$ $\bar{E}_\gamma = 2.8$ GeV

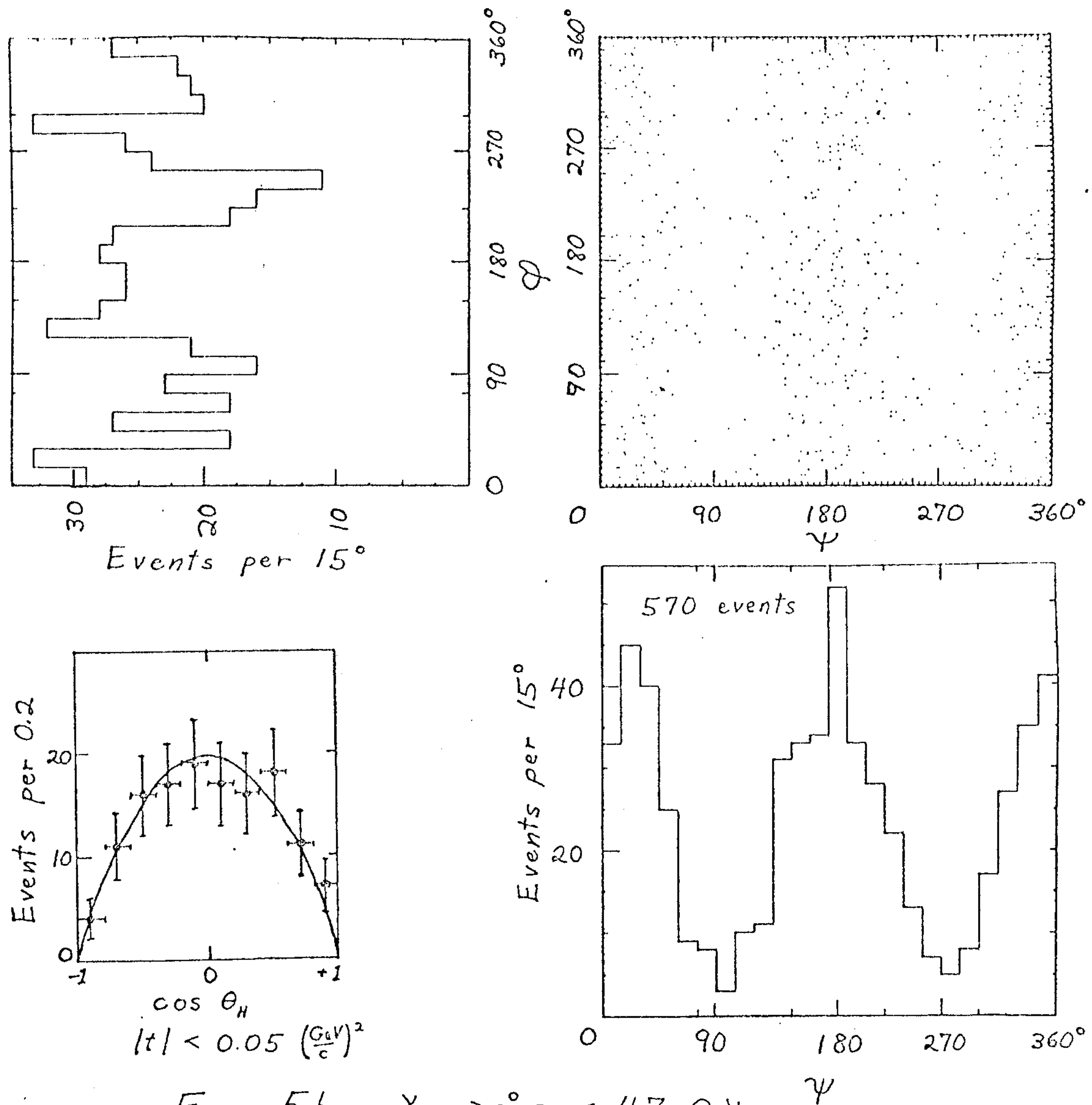

Fig. 5b $\gamma p \to \rho^{\circ} p$, $E_\gamma = 4.7$ GeV

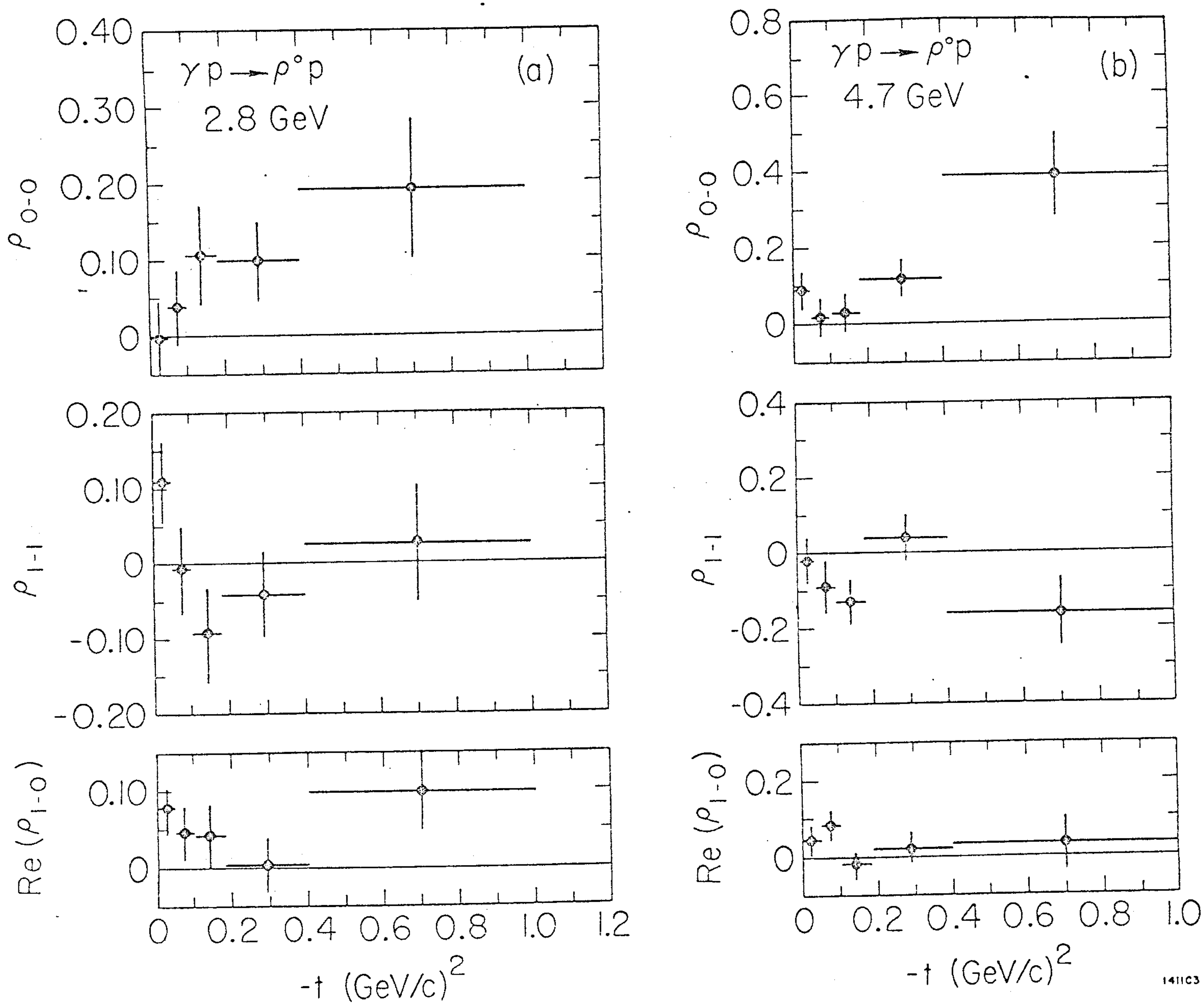

γp → ρ°p
2.8 GeV
(a)
γp → ρ°p
4.7 GeV
(b)
ρ0-0
ρ1-1
Re (ρ1-0)
-t (GeV/c)²
0 0.2 0.4 0.6 0.8 1.0 1.2
0 0.2 0.4 0.6 0.8 1.0
0.40 0.30 0.20 0.10 0
0.20 0.10 0 -0.10 -0.20
0.8 0.6 0.4 0.2 0
0.4 0.2 0 -0.2 -0.4
1411C3

FIG. 6

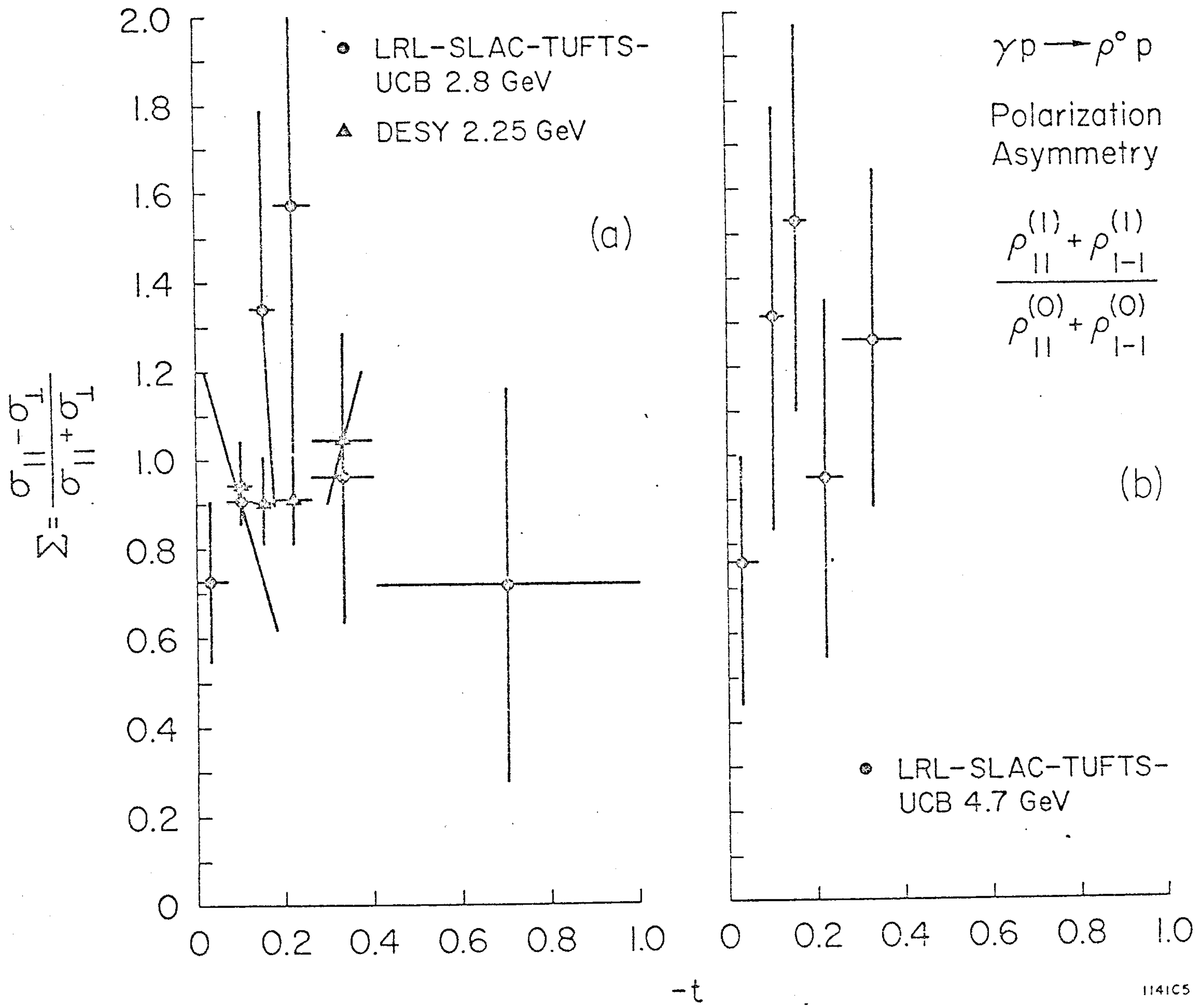
LRL-SLAC-TUFTS-UCB 2.8 GeV
DESY 2.25 GeV
(a)
$\Sigma = \frac{\sigma_{\parallel} - \sigma_{\perp}}{\sigma_{\parallel} + \sigma_{\perp}}$
$\gamma p \to \rho^{\circ} p$
Polarization Asymmetry
$\frac{\rho^{(1)}_{11} + \rho^{(1)}_{1-1}}{\rho^{(0)}_{11} + \rho^{(0)}_{1-1}}$
(b)
LRL-SLAC-TUFTS-UCB 4.7 GeV
-t
1141C5

FIG. 7

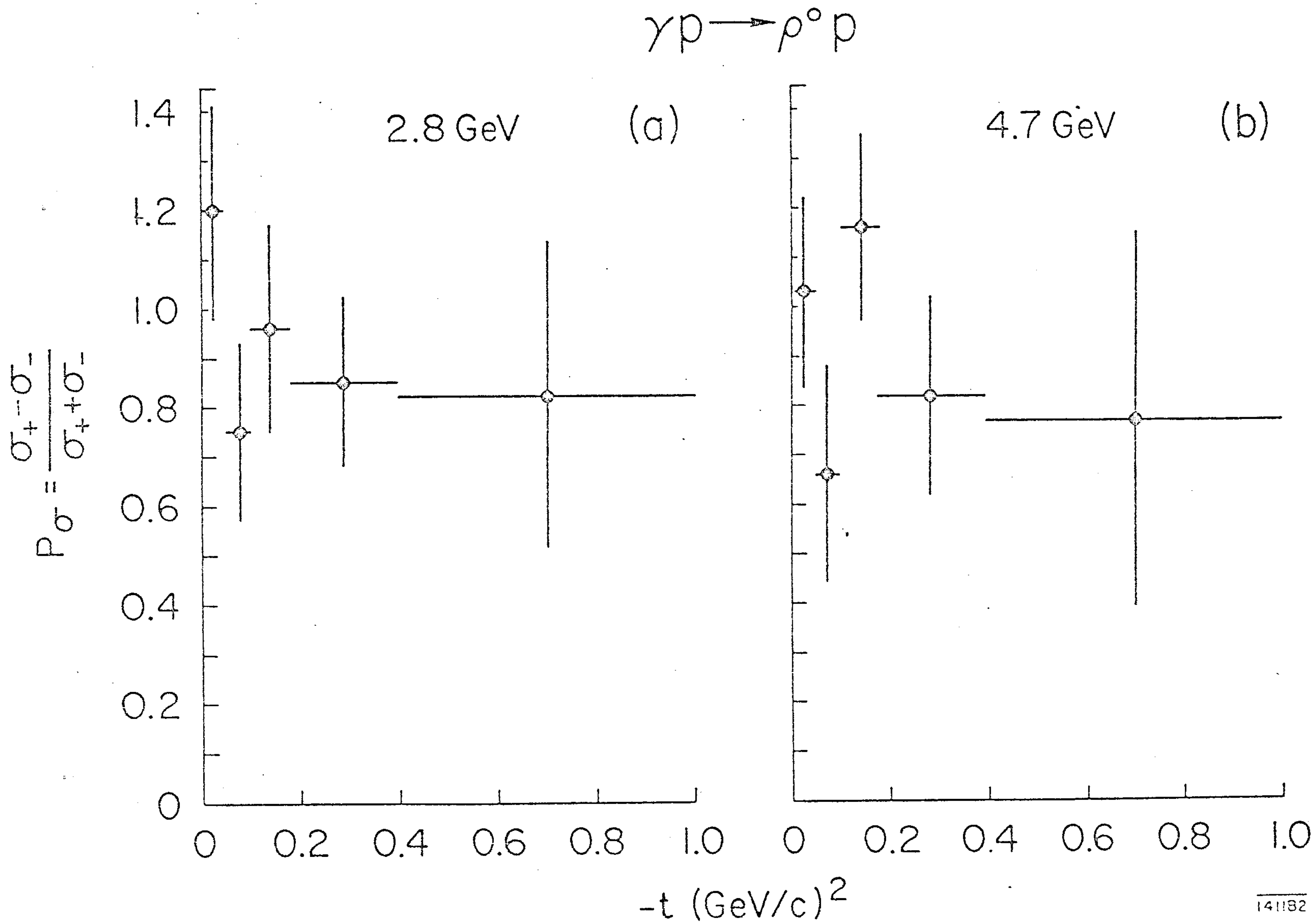
γp → ρ°p
2.8 GeV
(a)
4.7 GeV
(b)
$P_\sigma = \frac{\sigma_+ - \sigma_-}{\sigma_+ + \sigma_-}$
1.4
1.2
1.0
0.8
0.6
0.4
0.2
0
0
0.2
0.4
0.6
0.8
1.0
-t (GeV/c)^2
141182

FIG. 8

ϕ (FOLDED) DISTRIBUTION FOR STATISTICAL TENSOR Im T_2^2

(X) QUARK MODEL PREDICTION

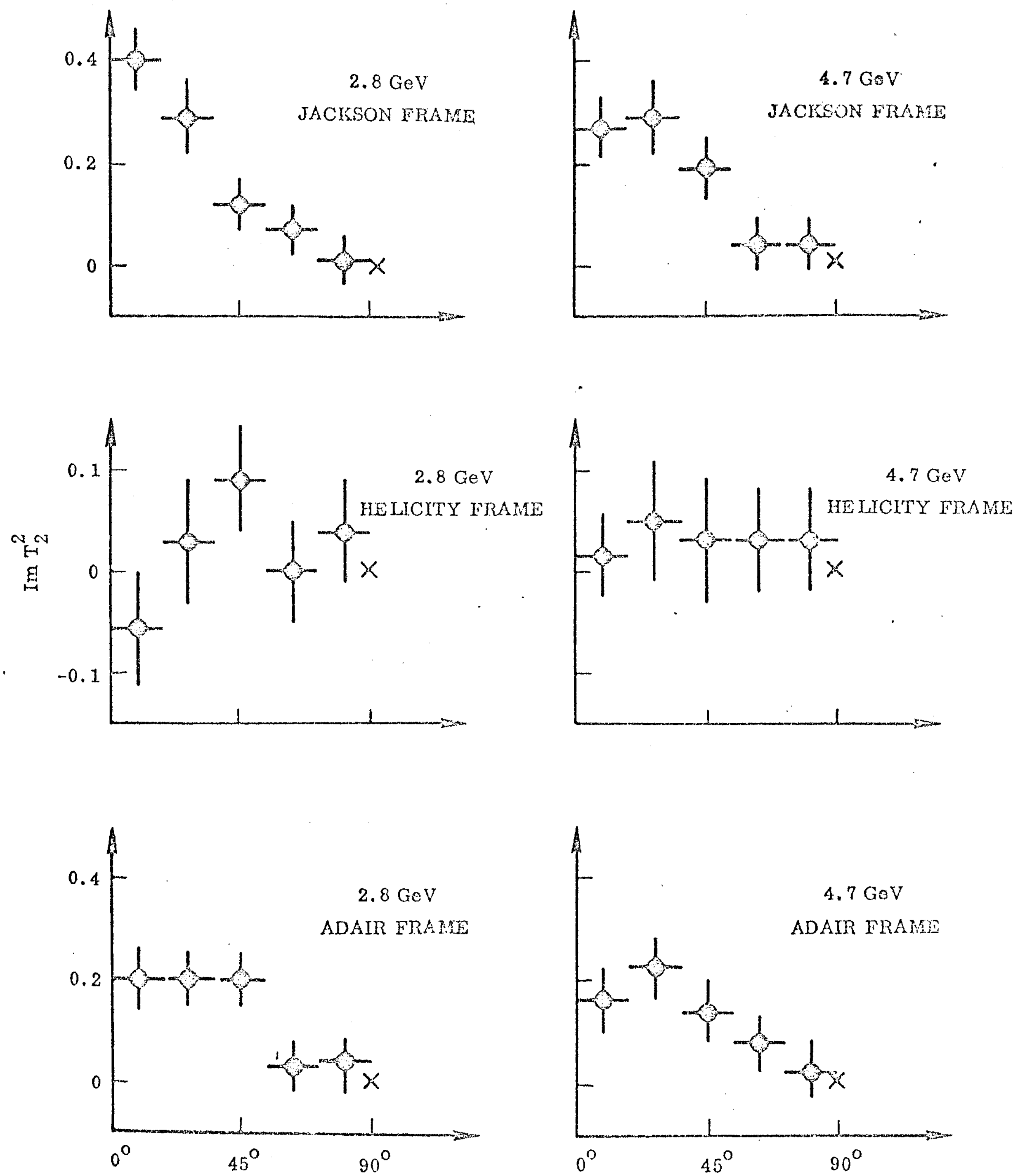

1411B1

FIG. 9